



Influence of magnesium and aluminium ions on the copper a.c. deposition into aluminium anodic oxide film nanotubes

A. JAGMINAS

Institute of Chemistry, LT-2600, A. Goštauto 9, Vilnius, Lithuania (fax: +370 2 61 70 18, e-mail: jagmin@ktl.mii.lt)

Received 13 June 2001; accepted in revised form 4 July 2002

Key words: aluminium, a.c. deposition, anodic oxide film, copper, magnesium

Abstract

The influence of Mg^{2+} and Al^{3+} ions on a.c. deposition of copper nanowires into aluminium anodic oxide film (AOF) nanotubes has been studied using cyclic voltammetry and d.c. plasma emission spectrometry. From the analysis of copper quantities deposited into the Al AOF nanotubes (m_{Cu}), 0.02 M $MgSO_4$ concentration was found to be optimal for Cu(II) solutions. Moreover, it was shown that Mg^{2+} and Al^{3+} ions not only prevent the breakdown of the barrier layer of AOF, but change the rate of copper deposition and modify the shape of the m_{Cu} against pH plots depending on the a.c. voltage applied. From the analysis of the quantities of magnesium (m_{Mg}) incorporated into the Al AOF nanotubes, presumably in the form of $Mg(OH)_2$, the m_{Mg} against pH dependences were determined in $MgSO_4$ and $MgSO_4 + CuSO_4$ solutions. An increase in m_{Mg} from $30 \mu g dm^{-2}$ to $1 mg dm^{-2}$ at pH 1.5 and from $6 \mu g dm^{-2}$ to $16 \mu g dm^{-2}$ at pH 7.0 was found under the same a.c. treatment conditions from $MgSO_4$ solutions without and with Cu^{2+} ions, respectively, indicating the incorporation of $Mg(OH)_2$ into the Al AOF nanotubes to be lower up to about one hundred times in the case of Cu deposition. Based on the experimental results, it was suggested that incorporation of the $Mg(OH)_2$ particles into the Al AOF nanotubes occurred simultaneously with growing copper nanowires under a.c. bias is insignificant, if the pH of the $CuSO_4 + MgSO_4$ solution is ≤ 2.5 .

1. Introduction

Self-ordered porous oxide films obtained by anodic oxidation of Al in acidic solutions have unique nanometre-sized honeycomb structures, composed of packed arrays of columnar hexagonal cells, each having a cylindrical nanotube (micropore) in the centre [1–3], normal to the Al substrate surface and separated from it by a thin barrier oxide film, which is impressed on the Al metal surface as a close-packed array of hemispherical cavities [4–6]. Excellent stability, insulating properties and the ability to design the Al anodic oxide films (AOF) with predetermined morphology make them potentially well-suited for use as templates for deposition of metals or semiconductors with high density nanoarrays. Deposition using a.c. methods of metal nanowire arrays into the Al porous AOF was used to produce deposits with interesting vertical magnetic [7–9], catalytic [10] and optical [11, 12] properties differing from those of the bulk metals. The metal nanowires faithfully reproduce the shape of the pores [13] with diameters ranging from 4 to 200 nm and length up to $100 \mu m$ [14]. Such nanochannel-array materials have stimulated considerable interest in recent years due to their utilization for nanometre devices [15, 16].

Deposition of metals into the Al AOF nanotubes is carried out preferentially by a.c. electrolysis without simultaneous material deposition on the film surface or into the macroscopic defects of the film. According to previous reports [7, 17], this is an ideal method for filling such nanotubes with metals, with deposition commencing at the bottom.

Copper deposited from acidic solutions [18] at the bottom of the Al AOF nanotubes [19–21], mainly in the metallic state, was found to be responsible for the cherry-colored AOF. Copper sulphate is most frequently used as a source of Cu^{2+} ions in quantities from 0.05 to 0.15 M. Either sulphuric or phosphoric acid is added to adjust the pH from 1.3 to 1.6 to increase the copper deposition uniformity and Mg^{2+} or Al^{3+} ions are used to prevent the breakdown of the AOF barrier layer [22].

It has been shown that copper can also be deposited into Al AOF nanotubes by a.c. electrolysis from Cu(II) acetate, citrate, ethanolamine and other solutions [23]. X-ray and FTIR analysis have shown that copper is deposited from these solutions only partially in the metallic state [24]. Both the composition and pH of the solutions govern the quantity of copper oxygen species in Cu_2O and CuO form. The general aspects of copper electrodeposition into Al AOF nanotubes from aqueous acidic $CuSO_4$ solutions have been discussed [25]. It has

been recognized that the rate of copper deposition decreases and a more intensive reddish color develops with decrease in solution pH. The greatest amount of copper can be deposited at pH 1.5, when the copper deposition rate is $2.2 \text{ mg dm}^{-2} \text{ min}^{-1}$ at an alternating current density $i_{\text{rms}} 0.4 \text{ A dm}^{-2}$. However, under these conditions, the Al AOF nanotubes are only partially filled with copper.

Sautter et al. [26] have suggested, on the basis of electron microscopy, that metallic copper rods of a few μm in length, deposited by the a.c. electrolysis from acidic copper sulphate solutions consist of separate crystals about 160 nm in length. Nevertheless, it has been suggested, that deposited copper can undergo a partial conversion to compound form [27, 28]. Our previous investigations [23, 24] have shown that the amount of these copper compounds depends essentially on the electrolyte acidity. The lower the pH of the electrolyte, the greater is the amount of metallic copper deposited into the Al AOF nanotubes and the lighter is the red finish obtained. Our latest studies of the copper a.c. deposition have revealed the influence of Mg and Al salts on the copper deposition rate and the codeposition of an insoluble magnesium compound [29]. Codeposition of Cu metal with Mg or Al hydroxides into the Al AOF nanotubes may be a serious problem for uniform filling of the pores and for quantum copper nanowire formation. Thus, the goal of this communication is to establish in more detail the role of Mg^{2+} and Al^{3+} ions in the copper nanowire deposition process.

2. Experimental details

2.1. Materials, specimen preparation and anodizing of Al surface

99.5% purity Al foil, containing Fe 0.24%, Si 0.2%, Cu 0.03%, Zn 0.02%, Ti 0.01% (trade mark AD0, Russia) of dimensions $50 \text{ mm} \times 50 \text{ mm} \times 0.075 \text{ mm}$ and $15 \text{ mm} \times 20 \text{ mm} \times 0.075 \text{ mm}$ were used for analytical and voltammetric investigations, respectively. In addition, a polycrystalline Al rod of purity 99.999% of the radius 0.565 cm, which was reduced to attain a final cross section of 1.0 cm^2 , was used for the $I(E)$ measurements. The cylindrical surface of the specimen was set into a Teflon sleeve. The working surface of the specimen was ground before each experiment using SiC emery paper. The surface of Al samples were decreased by soaking in ethanol for 10 min, rinsed with flowing water, etched in 1.5 M NaOH solution ($55 \pm 2 \text{ }^\circ\text{C}$, 60 s), rinsed with flowing water, desmutted in 1.5 M HNO_3 (60 s), then rinsed with distilled water. The specimens were anodized at 15 V d.c. voltage (U_a) in a stirred 1.53 M (15%) H_2SO_4 solution for 3 to 90 min by applying a current from a regulated power supply (0–40 V, 2.5 A, d.c. power supply TEC 23, Bulgaria). The electrolyte temperature was $20 \pm 0.2 \text{ }^\circ\text{C}$. Two pure lead plates were used as cathodes. Thus, oxide layers of different

thickness (δ_{AOF}), from 1.0 to 20 μm , having a barrier layer at the metal|oxide interface 15 nm in thickness (δ_b) and a porous layer, with oxide cells 37.5 nm in diameter and nanotubes 15 nm in diameter [1, 30] were formed on the Al surface. After anodizing, the samples were rinsed with flowing distilled water for 120 s, soaked for 30 s in triply distilled water to remove Al^{3+} ions remaining in the AOF pores after film growth and transferred immediately into the solution for the a.c. treatment.

2.2. Reagents

The chemicals used for the Al surface pretreatment (for degreasing, etching and desmutting) were reagent grade. Other solutions were prepared from high grade copper sulfate ($\text{CuSO}_4 \cdot 5\text{H}_2\text{O}$), magnesium sulfate ($\text{MgSO}_4 \cdot 6\text{H}_2\text{O}$), aluminium sulfate ($\text{Al}_2(\text{SO}_4)_3 \cdot 18\text{H}_2\text{O}$), nitric acid (HNO_3) and sulfuric acid (H_2SO_4) (from Aldrich) and triply distilled water. Before use, triethanolamine was distilled under vacuum at $200 \text{ }^\circ\text{C}$. Standard solutions used for analysis of Mg and Cu elements in concentration 1000 mg dm^{-3} were purchased from Merck.

2.3. Electrodeposition

After thorough rinsing, the anodized Al samples were subjected to electrolysis by sine wave a.c. bias of frequency 50 Hz at a constant average voltage (U_a) or at a constant voltage amplitude value (U_p) ranging from 5 to 28 V(rms) and centring around 0 V. Seven graphite rods 5 mm in diameter and 80 mm in length placed symmetrically around the sample were used as auxiliary electrodes. The following solutions were used: from 0.002 to 0.4 M MgSO_4 and from 0.005 to 0.4 M $\text{Al}_2(\text{SO}_4)_3$ without and with CuSO_4 in concentrations up to 1.1 M. The pH of the solutions was maintained at 1.0 to 8.0 using dilute H_2SO_4 (1:1) or triethanolamine–water (1:2) solution. pH was determined using a Mettler Toledo MP 220 pH meter. All treatments were performed at ambient temperature.

The gas evolved during the a.c. electrolysis at the anodized Al electrode was collected in an electrolyser as in [31]. The volume of the gas evolved was recalculated into the volume under standard conditions by the equation:

$$V_0 = V_1 T_0 (B_1 - W) B_0^{-1} T^{-1} \quad (1)$$

where V_0 is the gas volume under standard conditions ($T_0 0 \text{ }^\circ\text{C}$ and pressure $B_0 1.013 \times 10^5 \text{ Pa}$), V_1 is the gas volume measured at atmospheric pressure B_1 ; W is the water vapour pressure at the temperature of the experiment.

2.4. Electrochemical measurements

The experiments were performed in a conventional three-electrode one-compartment glass cell using a PI

50-1.1 potentiostat–galvanostat equipped with a PR-8 programmer and controlled by a personal computer, where data were collected, processed and analysed using software Mathead. In the electrochemical measurements, a Cu|Cu²⁺ electrode (99.99% purity Cu in 0.2 M CuSO₄ + 0.5 M H₂SO₄, 290 mV against RHE), placed in a separate cell compartment and connected to the working cell through a closed wet ground a stopcock and a Luggin capillary adjusted to within less than 1 mm from the surface of the working electrode was used as the reference. This electrode was chosen in order to have common ions with the bath solution. A graphite rod with about 4.0 cm² of geometric surface was employed as the counter electrode.

Voltammetric experiments were carried out at 0.05 to 10 V s⁻¹, scanning initially toward positive potentials up to +10 V. Only one cycle was run in each voltammetric experiment. The working compartment held approximately 75 cm³ solution. The temperature of the solutions was maintained at 20 °C with an accuracy of 0.2 °C by means of a water thermostat. Prior to use, all solutions were deoxygenated by bubbling pure Ar for about 30 min. All measured potentials equal to the potential difference between the Al electrode metallic core and the reference electrode [32] are given versus the standard hydrogen electrode (SHE).

2.5. Analysis

The samples assigned for the analysis of the deposits, incorporated into the Al AOF pores after a.c. bias treatment, were thoroughly rinsed in flowing distilled water and soaked in triply distilled water for 3 min to remove Cu²⁺ and/or Mg²⁺ ions remaining inside the pores. The quantities of copper and Mg(OH)₂, deposited into the Al AOF nanotubes, were determined after their dissolution from the surface of the smaller plates (4.5 cm²), obtained by cutting the initial specimen with dimensions 50 mm × 50 mm into the pieces with dimensions 15 mm × 15 mm. Dissolution was carried out in 5 cm³ of hot (75 ± 2 °C) HNO₃ (1:2) for 300 s. The conditions of the complete dissolution of copper from the pores of Al AOF have been determined earlier [25]. All solutions obtained were mixed together, diluted up to 50 or 100 cm³ and analysed quantitatively using a d.c. plasma emission spectrometer by comparison with standard solutions with a relative error less than 1%. The instrument used for this work was a Spectra-span-6 spectrometer (Beckman Instrument Co.), which employs a direct current argon plasma emission source and an echelle grating spectrometer to resolve the emitted light into the analytical wavelengths of Mg (279.55 nm) and Cu (327.40 nm) elements. Solutions for analysis were introduced to the plasma via a cross-flow nebulizer at a rate of 2.0 ml min⁻¹ by a peristaltic pump. Reproducibility of quantitative data was ascertained by repeating analyses four times and averaging the results.

3. Results and discussion

3.1. Influence of aluminium and magnesium ions on the copper electrodeposition

The results showed that copper can be deposited from aqueous acidic CuSO₄ solutions into the pores of Al AOF formed in H₂SO₄ electrolyte without destruction of the film at CuSO₄ concentrations 0.008 to 1.1 M and at an average a.c. voltage (U_v) of 6 to 13 V. At higher U_v values breakdown of the AOF barrier layer at the electrode edges leading to jumps of a current in the circuit was observed, resulting in a nonuniform AOF colouring. When the electrolysis was continued after initial breakdown was observed, or if it was performed at higher a.c. voltages, not only was a local breakdown of the AOF observed, but exfoliation of pieces of the film several mm² in size also occurred. In these solutions the resistance of AOF initially decreases and only after a specific amount of passed charge does it begin to increase.

If the CuSO₄ solution contained more than 0.005 M MgSO₄ or/and Al₂(SO₄)₃, the breakdown of the AOF during a.c. electrolysis was observed only at $U_v \geq 23$ V. As can be seen from the need to increase the a.c. voltage from the onset of electrolysis in order to maintain the same value of current, the resistance of the AOF increases as Cu is deposited. Considering these results, it can be suggested that the increase in Al AOF resistance in Cu(II) solutions containing Mg²⁺ or Al³⁺ ions may be related to codeposition of copper with magnesium or aluminium insoluble hydroxides at the bottom of the pores. It was found that Mg²⁺ and Al³⁺ ions have no effect upon the Al AOF tint, even when the concentration of the ions was increased up to 0.4 M. However, it was determined that, under the same a.c. electrolysis conditions the amount of deposited copper in the Al AOF pores depends on the concentration of Mg²⁺ or Al³⁺ ions in solution. In addition, it was established that the positive influence of Al³⁺ and Mg²⁺ ions on the process of copper electrodeposition at the bottom of the AOF nanotubes manifested itself not only with respect to the increase in the breakdown voltage, but also with respect to deepening of the oxide film color. Only in electrolytes containing Mg²⁺ (or Al³⁺) ions was it possible to fill the AOF nanotubes of thickness 15 to 20 μm right up to the oxide surface without breakdown of the film. As a consequence, the Al AOF was colored deep black and the surface of the film was covered by a finely dispersed copper visible to the naked eye.

3.2. Quantities of copper deposited into Al AOF nanotubes

The amount of copper (m_{Cu}) deposited into Al AOF nanotubes by a.c. electrolysis was found to be dependent on the concentrations of solution constituents, solution pH and on both the a.c. voltage and the duration of

electrolysis. At the same a.c. deposition conditions the m_{Cu} vs. pH dependence changed significantly when Mg^{2+} ions were added to the copper salt solution. The optimum concentration of MgSO_4 with respect to the highest rate of Cu deposition is 0.02 M, irrespective of the solution pH (Figure 1, curve 3). Additional experiments have shown that this is also true at different CuSO_4 concentrations. In the case of the solutions without Mg^{2+} or Al^{3+} , the amount of copper deposited under the same a.c. electrolysis conditions increased with increase in pH (curve 1). In the presence of Mg^{2+} , this amount was found to be independent of pH, when $U_v/U_a < 0.6$, that is, when the Al|AOF| Cu^{2+} electrode was in a weak a.c. field determining the low rate of Cu deposition (Figure 2(a)). Under the usual a.c. electrolysis conditions, when $0.7 < U_v/U_a < 1.0$, the m_{Cu} against pH dependence, as a rule, passed through a maximum at pH 1.5 (Figures 1 and 2(b)). At $U_v/U_a > 1.1$, the amount of copper deposited into the Al AOF nanotubes decreased progressively with increase in pH (Figure 2(c)). The shape of the m_{Cu} against pH plots changed if the Mg^{2+} ion concentration in the Cu(II) solutions was increased and U_v/U_a was equal to 0.6–0.7 or to 1.0–1.1. For example, it was established that, at U_v 9.0–10.5 V (U_v/U_a 0.6–0.7) the amount of deposited copper decreased progressively with increase in pH when $c_{\text{Mg}^{2+}} = 0.05$ M. The m_{Cu} against pH plot also depended on the duration of the a.c. electrolysis (Figure 2).

When the concentration of Al^{3+} ions ($c_{\text{Al}^{3+}}$) in Cu(II) solutions was increased up to 0.04 M, the amount of copper deposited into the Al AOF nanotubes remained almost unchanged provided the a.c. electrolysis conditions were held the same (Figure 3). For this reason, it was difficult to estimate the optimum concentration of Al^{3+} ions from the m_{Cu} against $c_{\text{Al}^{3+}}$ plots. However, the m_{Cu} against $c_{\text{Mg}^{2+}}$ and m_{Cu} against $c_{\text{Al}^{3+}}$ plots showed

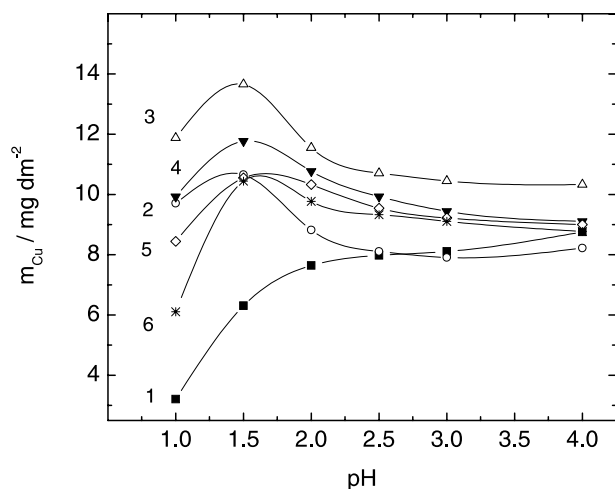


Fig. 1. Variation of the amount of copper deposited into Al oxide film nanotubes with electrolyte pH during 180 s a.c. treatment at $U_v = 12$ V and 20 °C in 0.1 M CuSO_4 solution, containing MgSO_4 (M): (■) 0; (○) 0.01; (△) 0.02; (▼) 0.03; (◇) 0.04; (※) 0.05. Oxide film thickness, $\delta_{\text{AOF}} = 10 \mu\text{m}$.

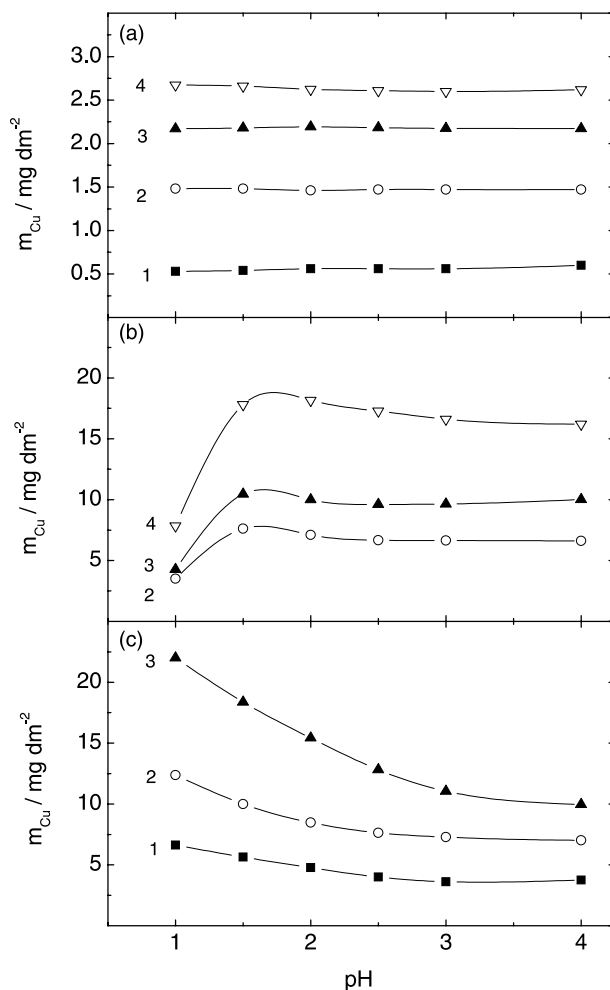


Fig. 2. Variation of the amount of copper deposited into Al AOF nanotubes from a solution of 0.1 M $\text{CuSO}_4 + 0.01$ M MgSO_4 with pH, as a function of a.c. voltage U_v (V): (a) 8, (b) 12, (c) 18 and electrolysis duration (s): (■) 60; (○) 120; (▲) 180; (▽) 300. $\delta_{\text{AOF}} = 10 \mu\text{m}$, 20 °C.

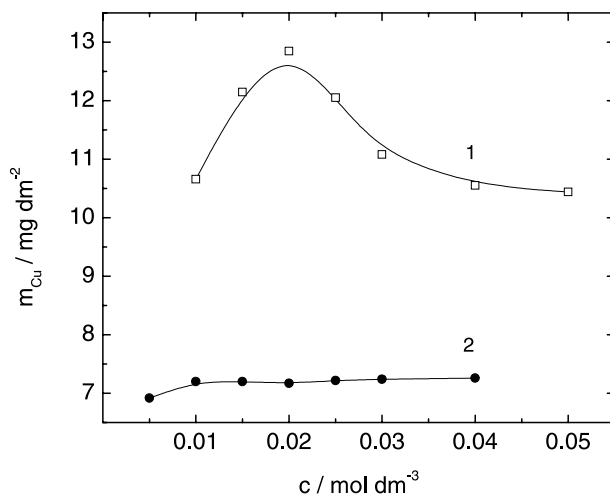


Fig. 3. Dependence of the amount of copper deposited into Al AOF nanotubes at $U_v = 12$ V and 20 °C over 180 s on MgSO_4 (□) and $\text{Al}_2(\text{SO}_4)_3$ (●) concentration in 0.1 M CuSO_4 solution. pH 1.5, $\delta_{\text{AOF}} = 12 \mu\text{m}$.

that the addition of MgSO_4 has advantages over $\text{Al}_2(\text{SO}_4)_3$ because, under the same electrolysis conditions, the amount of deposited copper in the presence of Mg^{2+} ions is up two times higher (Figure 3, curve 1). The m_{Cu} against pH dependence for CuSO_4 solutions containing Al^{3+} ions are presented in Figure 4. Their shape depends on the values of U_v . Up to $U_v = 11$ V, the amount of deposited copper progressively decreases with the increase in pH (Figure 4(a)). Meanwhile, for $U_v = 12$ – 15 V the m_{Cu} against pH plots usually have a maximum at pH 1.5, as in the case of Cu(II) solutions containing Mg^{2+} ions. The shape of the m_{Cu} against pH plots for these electrolytes at higher values of a.c. voltage ($U_v = 15$ V and more) was also found to be dependent on the duration of the a.c. electrolysis (Figure 4(c) and (d)). The differences in m_{Cu} against pH plots at different U_v values in the Cu(II) solutions containing Mg^{2+} (Al^{3+}) ions is related to changes in the relative contributions of the quantities of charge consumed for hydrogen evolution and copper deposition with increase in a.c. voltage, as predicted by Butler–Volmer theory for consecutive reactions [34]. On the other hand, deposition of the Mg(OH)_2 (Al(OH)_3) with

copper at higher U_v and pH should also change the rates of H_3O^+ and Cu^{2+} ion reduction occurring at the bottom of the pores.

3.3. Regularities of evolution of gaseous products

The amount of gaseous products evolved at the anodized Al electrode during a.c. electrolysis in aqueous solutions containing CuSO_4 , MgSO_4 or $\text{Al}_2(\text{SO}_4)_3$ depended, for the most part, on the applied voltage value and pH, increasing progressively with decrease in pH below 3.0 (Figure 5). At identical a.c. electrolysis conditions, the most gas was evolved from acidic ($\text{pH} \leq 1.75$) CuSO_4 solutions. Moreover, decrease in solution pH results in an increase in the uniformity of copper deposition into the Al AOF nanotubes simultaneously with a decrease in the amount of copper deposited (curve 1 in Figure 1). However, when Mg^{2+} or Al^{3+} ions were introduced to the CuSO_4 solution, the amount of gaseous products evolved was lowered from 2 to about 50 times at pH 2.5 and 1.5, respectively (curves 3 and 5 with respect to 1 in Figure 5). The minimum amount of the gas and the maximum amount of the

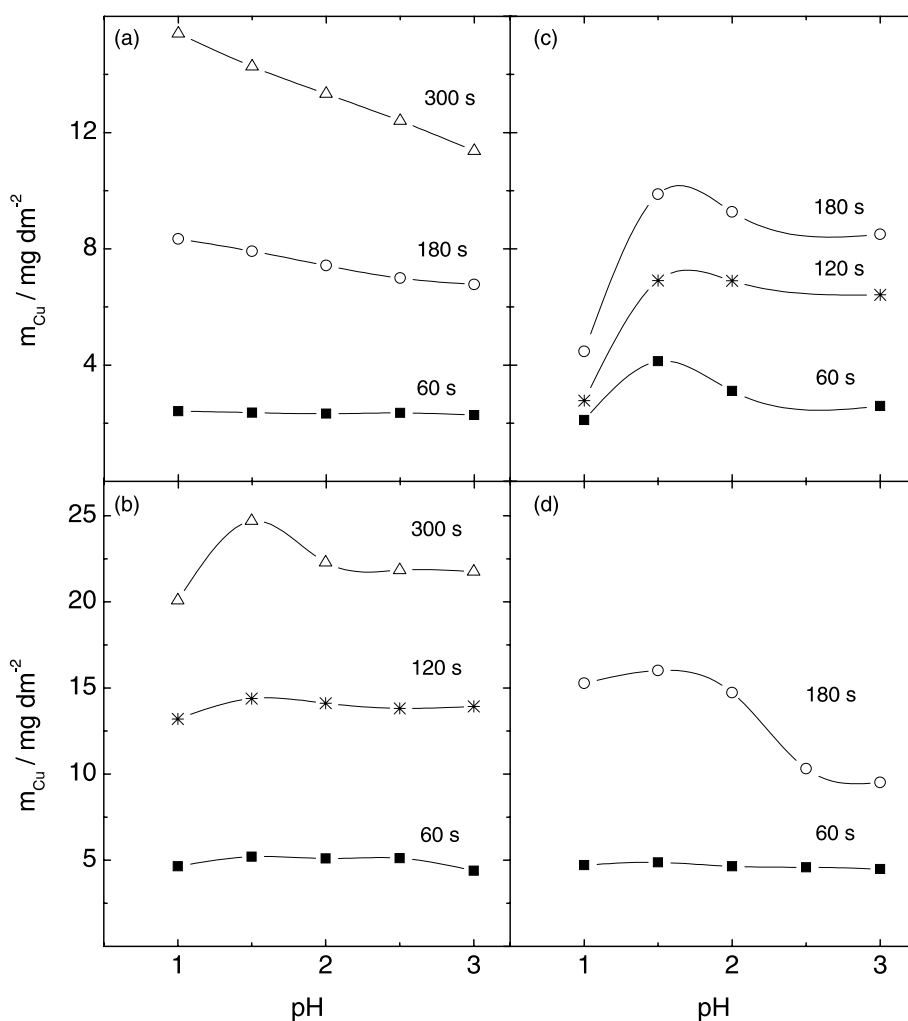


Fig. 4. Variation of the amount of copper deposited into Al AOF nanotubes from 0.1 M CuSO_4 + 0.02 M $\text{Al}_2(\text{SO}_4)_3$ solution at U_v (V): (a) 10, (b) 12, (c) 15, (d) 18 with pH and electrolysis duration. $\delta_{\text{AOF}} = 10 \mu\text{m}$, 20°C .

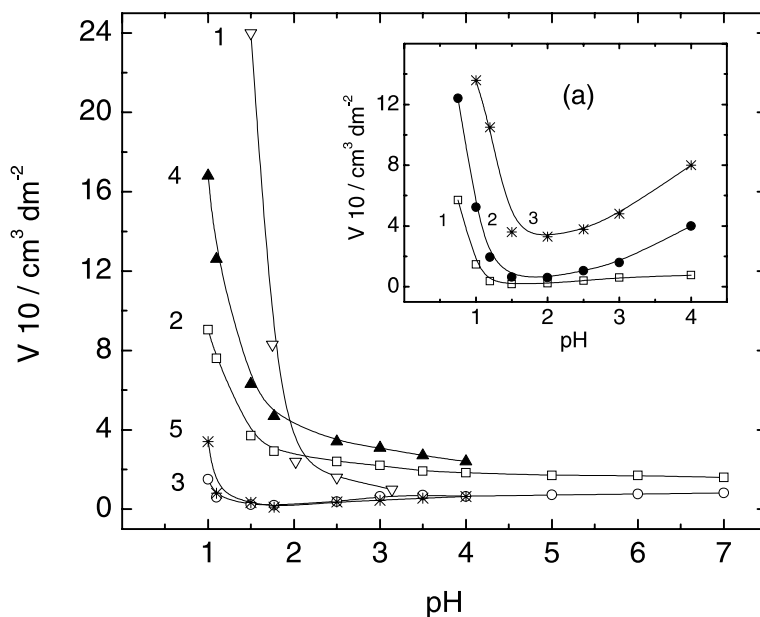


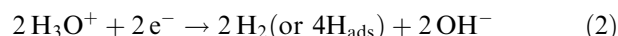
Fig. 5. Variations of the gas volume, evolved at anodized Al electrode during 300 s a.c. electrolysis at amplitude voltage (U_p) 15 V and 20 °C, with pH of the solution, containing (M): (∇) 0.1 CuSO₄, (\square) 0.02 MgSO₄, (\circ) 0.02 MgSO₄ + 0.1 CuSO₄, (\blacktriangle) 0.02 Al₂(SO₄)₃, ($*$) 0.02 Al₂(SO₄)₃ + 0.1 CuSO₄. (a) gas volume evolved under the same conditions in 0.1 M CuSO₄ + 0.02 M MgSO₄ at U_v (V): (1) 8, (2) 12, (3) 15. $\delta_{\text{AOF}} = 10 \mu\text{m}$.

copper deposited in CuSO₄ solutions containing Mg²⁺ or Al³⁺ was obtained at pH 1.5 to 2.0. This a dependence of the evolved gas on pH becomes increasingly more pronounced as the a.c. voltage increases (Figure 5(a)).

3.4. Codeposition of insoluble magnesium compounds with copper

As previous investigation of the electrolysis of the MgSO₄ solution under a.c. bias for Al|AOF|Mg²⁺ electrode has shown [29], appreciable evolution of hydrogen begins at about -6 V, reaching a peak current

at about -11.5 V. This leads to an increase in pH at the bottom of the Al AOF nanotubes by the reaction:



and, if pH is ≥ 2.5 , to the deposition of Mg(OH)₂. Further investigation of this phenomenon was carried out.

Variations of the amount of magnesium (m_{Mg}) incorporated into the AOF nanotubes with pH in the MgSO₄ and CuSO₄ + MgSO₄ solutions under identical a.c. treatments, are illustrated in Figure 6. Three regions can be defined for MgSO₄ solution (curve 1): the region A to

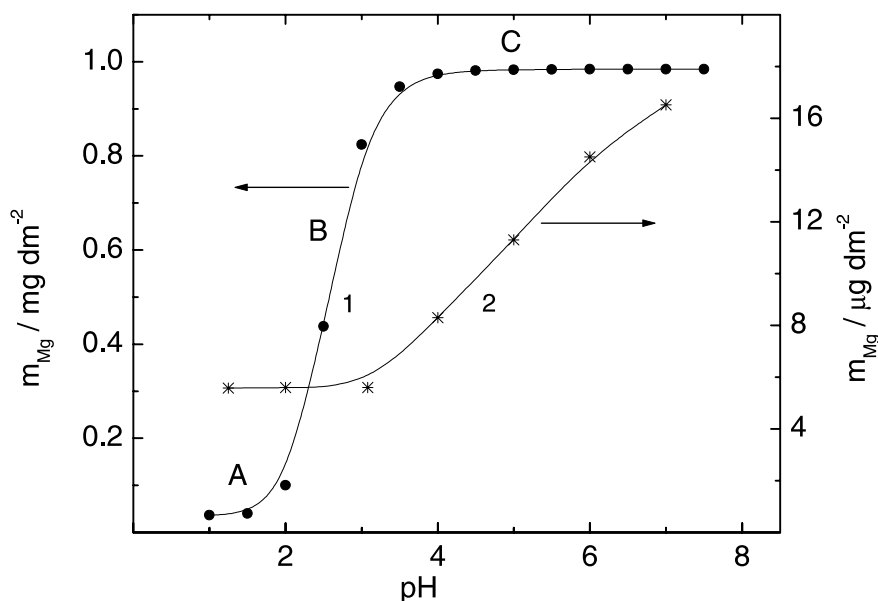


Fig. 6. Dependence of the amount of magnesium incorporated into Al AOF during 600 s a.c. electrolysis at $U_p = 15 \text{ V}$ and 20 °C on the pH and composition of electrolyte (M): (\bullet) 0.02 MgSO₄, ($*$) 0.02 MgSO₄ + 0.1 CuSO₄.

pH 2, where the amount of magnesium (m_{Mg}) is low, the region B between pH values from 2 to 3.5 of rapid increase in m_{Mg} and region C over pH 3.5 of steady high values of m_{Mg} . m_{Mg} increases with increasing a.c. voltage, however, the amount of magnesium incorporated at pH < 2.0 is still negligible. As seen in Figure 6 (curve 2), the incorporation of $\text{Mg}(\text{OH})_2$ into the Al AOF nanotubes in the $\text{MgSO}_4 + \text{CuSO}_4$ solution for identical a.c. treatment is about 100 times less than from solution without copper salt. The decrease in the amount of magnesium incorporated into the AOF may be associated with a lower rate of H_2 evolution because, if the amount of hydrogen evolved is decreased several times, the pH of the solution layer adjacent to the bottom of the AOF nanotubes increases to a lesser extent. However, the increase in the m_{Mg} incorporated into the Al AOF nanotubes from about $6 \mu\text{g dm}^{-2}$ at pH 2.5 to $16 \mu\text{g dm}^{-2}$ at pH 7.0 indicates that the codeposition of copper with $\text{Mg}(\text{OH})_2$ in increasing quantities takes place if solution pH is higher than 2.5.

3.5. Cyclic voltammetric responses during copper deposition

Several attempts have been made to use voltammetry and chronopotentiometry to study the behaviour of Al electrodes with porous oxide films in solutions of metal salts [35, 36]. Our previous study [36] has shown that voltammograms without a perceptible destruction of the oxide film can be recorded only under certain conditions, including the potential sweep rate, sweep route, and oxide film thickness. It was found here, that in acid $\text{Cu}(\text{II})$ solutions it is possible to record at least one current (I) against potential (E) profile to about -18 V leading to colouration of the oxide film if the potential

sweep rate (v) is higher than 0.1 V s^{-1} and the film thickness is $\geq 7.5 \mu\text{m}$. There is no significant difference between the behaviour of the AOF formed on 99.999% grade Al and that on 99.5% grade Al. However, the current densities at the same voltages are lower, when Al of higher purity is used.

The results obtained from the voltammetric experiments in acid $\text{Cu}(\text{II})$ solutions with and without Mg or Al salts are displayed in Figure 7. A rapid rise in current, related to hydrogen evolution at the metal-oxide interface beneath the pores [33], causes damage to the barrier layer: this occurs from the onset of the cathodic potential scan if Al or Mg salt is absent. No noticeable colouring of the oxide film and deposition of copper into the AOF nanotubes were observed in this case.

The voltammograms recorded in solution containing only MgSO_4 or $\text{Al}_2(\text{SO}_4)_3$ have one cathodic wave reflecting H_3O^+ reduction (Figure 8). H_3O^+ reduction begins below -5 V and reaches the peak current (i_p) at -9.5 to -11.5 V depending on solution concentration, pH, potential sweep rate, oxide film thickness (δ_{AOF}) and oxide film barrier layer thickness (δ_b). As seen in Figure 8(a) the cathodic peak current increases linearly with the square root of scan rate between 0.05 and 10 V s^{-1} , suggesting a diffusion-controlled process. In addition, as the pH increases, the slope of the linear i_p against $v^{0.5}$ plots decreases suggesting proton diffusion as a rate-determining step to be more pronounced at higher pH.

In the presence of Cu^{2+} ions the voltammograms became more complicated and consisted of more than one wave (Figure 7). The first wave was observed within the same potential range as in solutions without Cu^{2+} ions, indicating the first process to be proton reduction.

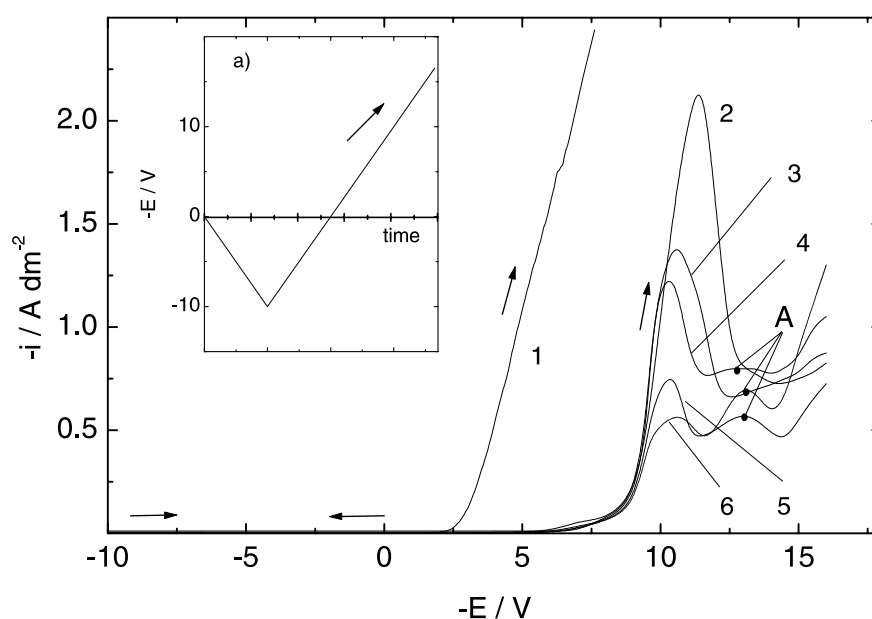


Fig. 7. Voltammograms of anodized aluminium electrode at $v = 0.2 \text{ V s}^{-1}$ in 0.1 M CuSO_4 solution (1) and in a solution, containing $0.08 \text{ M MgSO}_4 + 0.32 \text{ M H}_3\text{BO}_3 + \text{CuSO}_4$ (M): (2) 0, (3) 0.02, (4) 0.055, (5) 0.1, (6) 0.12. pH 4.0, $20 \text{ }^\circ\text{C}$, Al 99.5%, $\delta_{\text{AOF}} = 12 \mu\text{m}$. Insert: the routine of potential sweep.

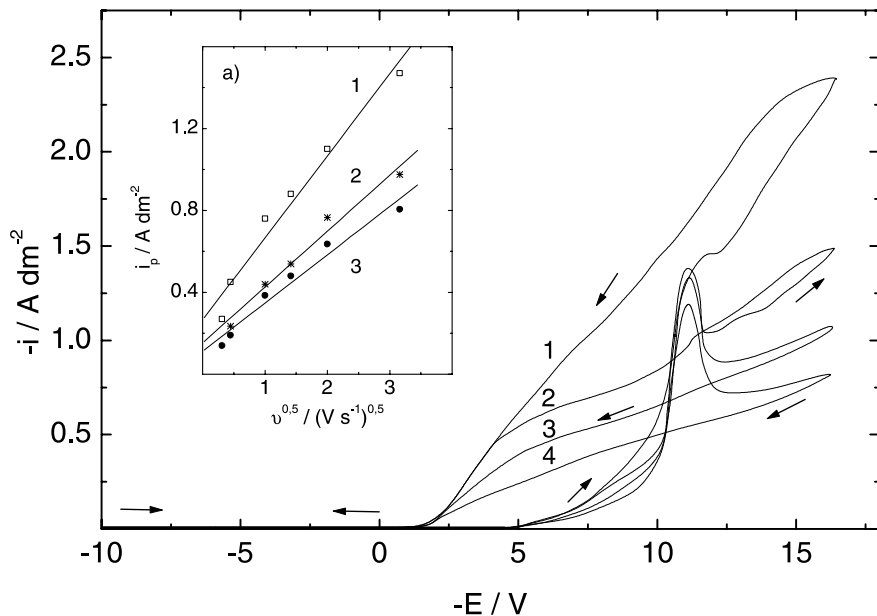


Fig. 8. Cyclic voltammograms of anodized aluminium electrode during potential sweep ($v = 0.2 \text{ V s}^{-1}$) in a solution, containing MgSO_4 (M): (1) 0.01, (2) 0.03, (3) 0.06, (4) 0.1 (pH 3.0). Insert: i_p against $v^{0.5}$ plots in the same electrolyte with $c_{\text{Mg}^{2+}} = 0.01 \text{ M}$ and pH: (1) 1.0, (2) 2.0, (3) 3.0. Al 99.999 %, $\delta_{\text{AOF}} = 10 \text{ }\mu\text{m}$, $20 \text{ }^\circ\text{C}$.

As confirmation of this, colouration of Al AOFs was observed only when the current peak of the second wave at about -13.5 V was reached. The current peak related to the H_3O^+ reduction increases and shifts to more positive potential with increasing $c_{\text{Mg}^{2+}}$ (Figure 9), however this increase is insignificant compared to the cathodic charge consumed up to the potential at which the second wave appears at point A (Figure 9(a)). Similar results were obtained in the Cu(II) acid solutions containing Al salts. Inhibition of the first cathodic reaction, marked as Δi in Figure 9, is related to

magnesium or aluminium salts. Δi increases with increasing $c_{\text{Mg}^{2+}}$ and $c_{\text{Al}^{3+}}$ and, presumably, may be associated with the adsorption or deposition of both copper and magnesium or aluminium hydroxides at the bottom of the oxide film nanotubes.

The current peak of the second wave (point A in Figure 7) is observed within the potential range from -12.5 to -15 V . It increases a little with increasing $c_{\text{Cu}^{2+}}$. Therefore, there are reasons to assume that the second current wave in the voltammograms, observed in solutions containing Cu^{2+} and Mg^{2+} or Al^{3+} ions, as well

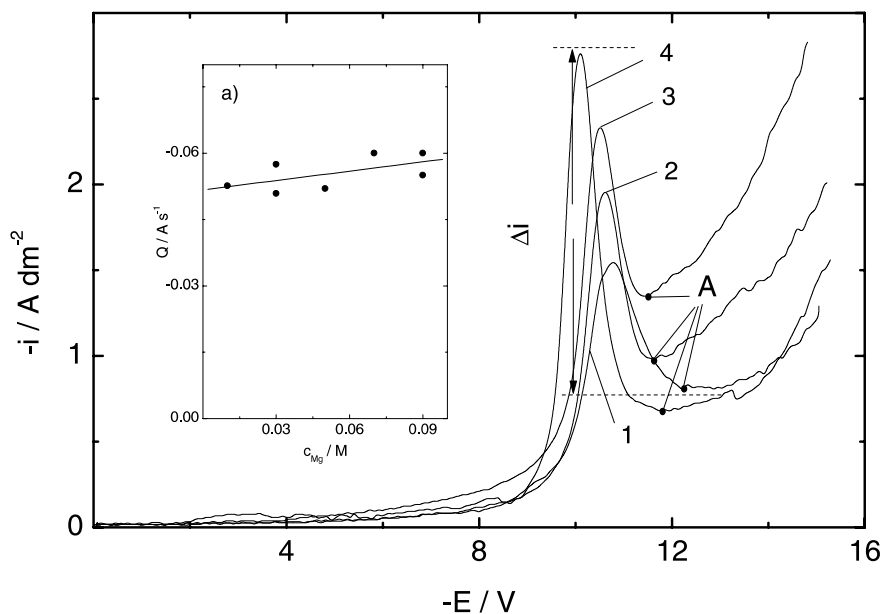


Fig. 9. Voltammograms recorded in the solution containing $0.1 \text{ M CuSO}_4 + \text{MgSO}_4$ (M): (1) 0.01, (2) 0.03, (3) 0.05, (4) 0.09 at $v = 0.6 \text{ V s}^{-1}$. $\delta_{\text{AOF}} = 9.0 \text{ }\mu\text{m}$, $20 \text{ }^\circ\text{C}$, Al 99.999% grade. Insert: dependence of the charge, corresponding to the first current wave, on the $c_{\text{Mg}^{2+}}$.

as other metal ions [35, 36], is related to the metal deposition at the bottom of Al AOF nanotubes. However, it was impossible to investigate the effect of both Mg^{2+} and Al^{3+} ions on the shape of the i_p against E plots at different v in the range of potentials of the second wave in acid Cu(II) solutions having different $c_{\text{Mg}^{2+}}$ and $c_{\text{Al}^{3+}}$, since the breakdown of the barrier part of oxide film occurred at $v \leq 1.5 \text{ V s}^{-1}$ or the first and the second polarization waves merged at $v > 1.5 \text{ V s}^{-1}$.

It is difficult to explain how Mg^{2+} or Al^{3+} ions influenced the discharge of Cu^{2+} ions at the bottom of oxide film nanotubes and prevented the breakdown of the oxide film at much higher a.c. voltages. On the basis of the experimental data, it may be concluded that the effect of these ions on oxide film breakdown prevention may be attributed to the strong inhibition of hydrogen evolution, especially at $\text{pH} \leq 1.5$ (Figure 5), due to a layer of Mg or Al hydroxides deposited or adsorbed at the bottom of the Al AOF nanotubes. The formation of $\text{Al}(\text{OH})_3$ or $\text{Mg}(\text{OH})_2$ in the solution bulk at the bottom of oxide film nanotubes should depend on the concentration of these ions and on the magnitude of the cathodic potential, which effects the reduction of Cu^{2+} ions. This was confirmed by the data presented in Figures 2 and 4.

4. Conclusions

It was determined that Mg^{2+} and Al^{3+} ions not only prevented the breakdown of the Al anodic oxide film (AOF) during a.c. treatment, but also blocked to a great extent hydrogen evolution, changing the amount of copper deposited rather than the shape of the m_{Cu} against pH plots. The dependence of m_{Cu} on pH and composition of the solution was found to be as follows: (i) in Cu(II) solutions without Mg^{2+} (Al^{3+}) ions, the amount of Cu deposited into Al AOF nanotubes increased with pH; (ii) in Cu(II) solutions containing Mg^{2+} or Al^{3+} ions, the shape of the m_{Cu} against pH plots changed and these dependences most often passed through a maximum at pH 1.5; (iii) under the same a.c. electrolysis conditions, the amount of copper deposited into AOF nanotubes from $\text{CuSO}_4 + \text{MgSO}_4$ ($\text{Al}_2(\text{SO}_4)_3$) solutions depended not only on the solution composition but also on U_v/U_a ; (iv) the optimum MgSO_4 concentration (most likely, that of $\text{Al}_2(\text{SO}_4)_3$ as well) with respect to the highest rate of Cu deposition was 0.02 M. The amount of magnesium incorporated as $\text{Mg}(\text{OH})_2$ into AOF nanotubes in the presence of Cu^{2+} ions under the same a.c. electrolysis conditions was found to be about 100 times lower. Moreover, it is suggested that only traces of $\text{Mg}(\text{OH})_2$ were incorporated into Al AOF nanotubes simultaneously with growing copper nanowires under a.c. bias in $\text{CuSO}_4 + \text{MgSO}_4$ solution at $\text{pH} \leq 2.5$.

Acknowledgement

The author is indebted to Dr Algirdas Selskis of the Institute of Chemistry in Vilnius, for performing the d.c. plasma emission spectrometry. The present work was supported by a grant-in-aid from the Lithuanian State Foundation for Science and Studies (No. T-465).

References

1. J.P. O'Sullivan and G.C. Wood, *Proc. Roy. Soc. Lond.* **A317** (1970) 511.
2. J.A. Switzer, C.J. Hung, B.E. Breyfogle, M.G. Shumsky, R.V. Leeuwen and T.D. Golden, *Science* **264** (1994) 1573.
3. H. Masuda and K. Fukuda, *Science* **268** (1995) 1466.
4. F. Keller, M.S. Hunter and D.L. Robinson, *J. Electrochem. Soc.* **100** (1953) 411.
5. L. Young, 'Anodic Oxide Films' (Academic Press, London, 1961).
6. J. Diggle, T. Downie and C. Goulding, *Chem. Rev.* **69** (1969) 365.
7. S. Kawai and R. Ueda, *J. Electrochem. Soc.* **122** (1975) 32.
8. D. All-Mawlawi, N. Coombs and M. Moskovits, *J. Appl. Phys.* **70** (1991) 4421.
9. D.J. Dunlop, S. Xu, Ö. Ördemir, D. All-Mawlawi and M. Moskovits, *Phys. Earth Planet Inter* **76** (1993) 113.
10. D. Miller and M. Moskovits, *J. Am. Chem. Soc.* **111** (1989) 9250.
11. C.K. Preston and M. Moskovits, *J. Phys. Chem.* **97** (1993) 8495.
12. M. Saito, M. Kirihara, T. Taniguchi and M. Miyagi, *Appl. Phys. Lett.* **55** (1989) 607.
13. K. Douglas, G. Devaud and N.A. Clark, *Science* **257** (1992) 642.
14. H. Masuda, H. Yamada, M. Satch, H. Asch, M. Nakao and T. Tamamura, *Appl. Phys. Lett.* **71** (1997) 2770.
15. G.H. Pontifex, P. Zhang, Z. Wang, T.L. Haslett, D. All-Mawlawi and M. Moskovits, *J. Phys. Chem.* **95** (1991) 9989.
16. D. Routkevich, A.A. Tager, J. Haruyama, D. All-Mawlawi, M. Moskovits and J.M. Xu, *IEEE Trans. Electron Devices* **43** (1996) 1646.
17. D.G. Goad and M. Moskovits, *J. Appl. Phys.* **49** (1978) 2929.
18. W. Sautter, G. Ibe and J. Meier, *Aluminium* **50** (1974) 143.
19. J. Patrie, *Trans. IMF* **53** (1975) 28.
20. P.G. Sheasby and W.E. Cooke, *Trans. IMF* **55** (1977) 119.
21. C.K. Preston and M. Moskovits, *J. Phys. Chem.* **92** (1988) 2957.
22. E. Hermann, *Galvanotechnik* **63** (1972) 110.
23. A. Jagminas and J. Giedraitienė, *Chemija* (Vilnius) **9** (1998) 55.
24. A. Jagminas and J. Giedraitienė, *Elektrokhimiya* (Russia) **36** (2000) 413.
25. A. Jagminas and J. Rėklaitis, *Zashch. Met.* **22** (1986) 821.
26. W. Sautter, G. Ibe and J. Meier, *Aluminium* **50** (1974) 143.
27. E. Lichtenberger-Bazja, F. Dömölki and I. Imre-Boan, *Metal Finish.* **71** (1973) 50.
28. S. Ishida and G. Ito, *J. Met. Fin. Soc. Jpn.* **40** (1989) 1394.
29. A. Jagminas, S. Lichušina and A. Selskis, 50th ISE Meeting Abstracts, Pavia, 5–10 Sept. (1999), p. 488.
30. Y. Fukuda, T. Takushima and M. Nagayama, *J. Met. Fin. Soc. Jpn.* **35** (1984) 513.
31. A. Jagminas, J. Giedraitienė and A. Selskis, *Chemija* (Vilnius) **11** (2000) 3.
32. G. Patermarakis and K. Moussoutzianis, *Electrochim. Acta* **40** (1995) 699.
33. J. Gruberger and E. Gileadi, *Electrochim. Acta* **31** (1986) 1531.
34. R. Brdička, *Grundlagen der Physikalischen Chemie*, 12 Auflage, Berlin (1973).
35. T. Sato and S. Sakai, *Trans. IMF* **57** (1979) 43.
36. V. Skominas, S. Lichušina, P. Miečinskas and A. Jagminas, *Trans. IMF* **79** (2001) 213.